Possible regulation of the immune modulator tetraspanin CD81 by alpha-synuclein in melanoma

Nirjhar M. Aloy[1,2], Christina Coughlan[3], Michael W. Graner[3], and Stephan N. Witt[1,2*]

[1]Department of Biochemistry and Molecular Biology, Louisiana State University Health Sciences Center, Shreveport, LA, USA. [2]Feist-Weiller Cancer Center, Louisiana State University Health Shreveport, Shreveport, USA. [3]University of Colorado Anschutz Medical Campus, Denver, CO, USA.

*To whom correspondence should be addressed: Tel: 318-675-7826; Fax: 318-675-5180; E-mail: stephan.witt@lsuhs.edu

Keywords: alpha-synuclein, CD81, melanoma, Parkinson's disease, tetraspanin

Abbreviations

BRCA, Breast invasive **c**arcinoma

CXCL13, C-X-C chemokine ligand 13

CRISPR, clustered regularly interspaced short palindromic repeats

EV, extracellular vesicles

FPKM, fragments per kilobase of exon per million mapped reads

GZMB, granzyme B

HPA, human protein atlas

IHC, immunohistochemistry

IL, interleukin

IFNG, interferon gamma

KI, knockin

KO, knockout

LUAD, lung adenocarcinoma

NK, natural killer cells

NTA, nanoparticle tracking analysis

PAAD, pancreatic adenocarcinoma

PCAWG, pan-cancer analysis of whole genomes

PD, Parkinson's disease

PRF1, perforin 1

SKCM, cutaneous melanoma

TCGA, the cancer genome atlas program

UVB, ultraviolet B

Abstract

Herein we probed the mechanism by which α-syn/*SNCA* promotes the pathogenesis of melanoma. We found that SK-MEL-28 *SNCA*-KO melanoma clones have very low levels of tetraspanin CD81, which is a cell-surface protein that promotes invasion, migration, immune suppression. Analyzing data from the Cancer Genome Atlas, we show that *SNCA* and *CD81* mRNA levels are positively correlated in melanoma; melanoma survival is inversely related to the levels of *SNCA* and *CD81*; and *SNCA*/*CD81* is inversely related to key cytokine genes (*IFNG*, *CXCL13*, *PRF1* and *GZMB*) for immune activation and immune cell-mediated killing of melanoma cells. We propose that high levels of α-syn help melanoma cells evade the immune response.

Introduction

Parkinson's disease (PD) is a progressive neurodegenerative disease in which midbrain dopaminergic neurons die, which leads to disturbances in gait and balance and the development of resting tremor [1]. Cancer is a disease of uncontrolled cell growth [2]. Although PD and cancer would seem to be unrelated, individuals with PD appear to be protected from all cancers except melanoma and brain cancer [3-5]. The co-occurrence of PD and melanoma is fueling a variety of studies to understand the molecular basis for this phenomenon. A recent meta-analysis of 63 publications, which included data obtained from over 17 million individuals, confirmed an inverse relation between PD and cancer, i.e., individuals with PD have a 15% lower risk of developing cancer, whereas individuals with cancer have a 26% lower risk of developing PD [6]. Strikingly, individuals with PD have a 75% higher risk of melanoma [6]. Several genes, including *Parkin*, *SNCA*, *DJ-1*, *LRRK2*, *Sox6* have been suggested to be involved in the co-occurrence of these two very different diseases [7-9]. Our focus here is *SNCA*, which codes for the presynaptic protein alpha-synuclein (α-syn), which is highly expressed in neurons and melanocytes [10].

α-syn is an intrinsically unfolded protein [11] in solution that adopts an α-helical conformation when it binds to membranes enriched with negatively charged phospholipids (PL) such as phosphatidylserine and phosphatidic acid [12, 13]. Due to an internal hydrophobic domain, synuclein self-associates into a plethora of soluble oligomeric species, as well as insoluble amyloid fibers [14]. Some of these soluble oligomers or soluble amyloid fragments are likely the cytotoxic species that cause neurodegeneration in synucleinopathies like PD [15], dementia with Lewy bodies, and

multiple system atrophy. In neurons, α-syn promotes SNARE complex assembly [16] and dilation of exocytic fusion pore [17].

In melanoma, α-syn functions in autophagy [18], melanin synthesis [19], and vesicular trafficking [20]. For example, α-syn inhibits the UVB light-induced increase in melanin synthesis, consequently melanin content is lower when melanoma cells express α-syn [19]. This implies that robust α-syn expression makes melanocytes more susceptible to UV-induced radiation damage. Loss of α-syn expression in cutaneous melanoma cells results in decreased levels of cell surface proteins such as the transferrin receptor and the adhesion proteins L1CAM and N-cadherin [20]. One possibility is that α-syn promotes anterograde trafficking of cell surface proteins; thus, loss of α-syn expression blocks these pathways and instead these proteins are shunted to the lysosome.

Here we report that loss of α-syn expression in SK-MEL-28 cutaneous melanoma cells results in a significant decrease in the level of the cell-surface protein CD81. CD81 is a member of the tetraspanin family [21] and is frequently used as a marker for extracellular vesicles (EVs) [22]. Emerging evidence suggests that CD81 has a critical role in the progression of breast cancer [23, 24] and melanoma [25, 26]. Specifically, it was reported to promote invasion and migration [23] and immune suppression through the regulation of Treg and myeloid-derived suppressor cells in breast cancer [27]. A previous study from our lab showed that cell migration was significantly decreased in SK-MEL-28 *SNCA*-KO melanoma cells, but the mechanism was not completely understood. We suggest that the reduced migration and motility of SK-MEL-28 *SNCA*-KO cells is also related to the loss of CD81 expression, and that α-syn regulates the

level of CD81. Additionally, we present evidence that α-syn and CD81 promote the pathogenesis of melanoma by suppressing the immune response.

Materials and methods

Cell Lines and Cell Culture

SK-MEL-28 cells were purchased from ATCC (Catalog number HTB-72). *SNCA* was knocked out in our lab using CRISPR-Cas9 [28]. α-syn expression was rescued in KO8 and KO9 clones using lentivirus constructs, and the 'knock-in' clones were named KI8 and KI9, respectively. Control, KO8, KO9, KI8, and KI9 clones of SK-MEL-28 melanoma cells were cultured and maintained at 37°C in Dulbecco's Modified Eagle's Medium (DMEM, ATCC-30-2002) that was supplemented with 10% exosome-depleted fetal bovine serum (Exo-FBS, Systems Bioscience) and 1% penicillin-streptomycin.

RNA extraction and RT-qPCR

SK-MEL-28 cells were grown for 48 hours at 37°C, at 5% CO2 in complete DMEM medium. Total RNA was extracted using E.Z.N.A total RNA kit I (Omega Boi-Tek, cat.-R6834-02) following the manufacturer's protocol. RNA quality and concentration was assessed with NanoDrop 2000c (Thermo Scientific). cDNA was synthesized from 1 µg of total RNA from each sample as follows: 1 µg total RNA + 2 µL 5X first strand buffer + 1 µL DNAse I + DEPC treated ddH2O to make 10 µL total volume. This was incubated for 30 minutes at 37°C. Then, 1 µL of DNAseI-DNAse I-inhibitor was added and incubated at 65°C for 10 minutes and quenched on ice for 1 minute. The reverse transcription reaction was set up as follows: 5 µL DNAase treated RNA+1 µL 5X RT buffer + 0.25 µL random primers (1:30 dilution) + 0.25 µL dNTPs + 0.5 µL DTT + 0.2 µL

RNAse-inhibitor + 0.2 µL MMLV RTase (Promega, cat. no. M1708) or (ddH20 for RT-) + 2.6 µL DEPC treated ddH2O = 10 µL final volume of mastermix was incubated at 37°C for 1 hour. This reaction was incubated at RT with a no primer control for each sample to ensure that there was no non-specific amplification in the qPCR reaction. Finally, the samples were treated with RNAseH at 37°C for 30 minutes.

qPCR was performed using the iTaq Universal SYBR Green Supermix (Bio-Rad, Cat. #1725121) according to the manufacturer's protocol. Primers (Int. DNA Tech.):

CD81 Forward: 5'-CAAGTACCTGCTCTTCGTCTTC-3'.

CD81 Reverse- 5'- TTGTCTCCCAGCTCCAGATA-3'.

Actin: Forward: 5'-GGAGAAGAGCTACGAGCTGCCTGAC-3'

Actin Reverse: 5'-AAGGTAGTTTCGTGGATGCCACAGG-3'

Western Blotting

SK-MEL-28 control, KO8, K09, KI8, KI9 cells were cultured for 48 hours in Dulbecco's Modified Eagle's Medium (DMEM, ATCC-30-2002) supplemented with 10% exosome depleted fetal bovine serum (Exo-FBS, Systems Bioscience) and 1% penicillin-streptomycin. After two washes with ice-cold PBS, cells were lysed in ice-cold RIPA buffer, and after passing through a 25G needle, the cell lysates were centrifuged at 18,360 g at 4°C for 20 minutes. Protein concentration was determined using the BCA protein assay (Thermofisher, Cat- 23250). Equal amounts of protein were loaded into each lane of NuPAGE™ 4-12%, Bis-Tris mini protein gels (ThermoFisher, Cat-NP0336PK2) and PAGE was performed at constant voltage (170 watts). Semi dry

transfer to nitrocellulose blots was performed using Trans blot Turbo (Biorad, Cat 1704150). After one hour of blocking in membrane blocking agent (G-Biosciences, Cat-786-011), incubation with primary antibodies was done overnight at 4°C. After washing the membranes 5 times (5 minutes each) with PBST, incubation with secondary antibody was performed at room temperature. Western blot images were acquired using chemiDoc Touch machine (Biorad). The protein concentration of EV samples was determined using the BCA protein assay. EV samples were lysed with NuPAGE SDS sample buffer (Invitrogen, Cat – NP0007), and 20 µg of EV-protein was loaded into each lane of the polyacrylamide gel, and Western blotting was performed as described above. In some cases, membranes were stripped (G Biosciences, Cat- 786-305), cut into pieces, and the pieces were re-probed (Fig. S2).

Isolation of EVs

Control, KO8, KO9, KI8, and KI9 clones of SK-MEL-28 melanoma cells were grown in the media as mentioned above for 48 hours in T-75 flasks. 10 ml of conditioned media was collected from each flask and centrifuged at 3,000 g for 15 minutes to pellet live and dead cells, cell debris, and large microvesicles. The supernatant was collected for EV-isolation. 2 mL of ExoQuick TC ULTRA (Cat- EXOTC10A-1) reagent was added to the supernatant at 1:5 ratio and EVs were isolated using the manufacturer's protocol.

Nanoparticle tracking

The EV-samples were preserved in Buffer B (Systems Bioscience) at -80°C and sent to the University of Colorado Anschutz Campus for nanotracking particle analysis (NTA).

The size distributions of EVs were determined by NTA Nanosight device (NS300, Software Version: NTA 3.2 Dev Build 3.2.16; Malvern Panalytical, Malvern WR14 1XZ, UK). One ml of exosome sample was prepared by freshly diluting the exosome sample 1:1000; and 1:10,000 in ddH2O (0.1µm filtered) before reading. Exosome number was captured using the following analytical settings on the NTA: camera type: sCMOS, level 5 (NTA 3.0 levels); green laser; slide setting and gain: 600, 300; shutter: 15 ms; histogram lower limit: 0; upper limit: 8235; frame rate: 24.9825 fps; syringe pump speed: 25 arbitrary units; detection threshold: 7; max jump mode: auto; max jump distance: 15.0482; blur and minimum track length: auto; first frame: 0; total frames analyzed: 749; temp: 21.099-22.015 °C; viscosity: 1.05 cP.

Reagents and antibodies

ExoQuick-TC® ULTRA for the isolation of exosomes from Tissue Culture Media (EQULTRA-20TC-1; System Biosciences). Antibodies used were all mouse primary monoclonal antibodies: anti human CD81 (1:500, Santa Cruz Biotechnology), CD63 (1:500, Abcam), HSP70/HSP72 (1:1000, Enzo, C92F3A-5), α-syn (1:1000, Santa Cruz Biotechnology), α-Tubulin (1:4000, Sigma Aldrich). Rabbit primary polyclonal antibodies: human CD9 (1:500, Systems Bioscience, # EXOAB-CD9A-1), HSP90 Antibody (1:1000, Cell Signaling Technology #4874). Mouse and rabbit secondary antibodies (1:2000, Santa Cruz Biotechnology).

Bioinformatics

The correlation between *SNCA* and *CD81* mRNA abundance was generated from the RNAseq data from the TCGA PanCancer Atlas datasets using the interactive platform of cBioportal. The raw data can be downloaded from cBioportal (https://www.cbioportal.org/). *CD81* expression across 17 cancer types was determined by analyzing the RNAseq data from TCGA (n=7932, Human Pathology Atlas), obtained through the Human Protein Atlas database (HPA) [accessed on 2/22/24]. The number of samples from each cancer type can be obtained from: https://www.proteinatlas.org/about/assays+annotation#tcga_rna_seq_data.
The gene expression values were expressed in FPKM (Fragments Per Kilobase of exon per Million mapped reads). The box plots were generated using the interactive graphical interphase of HPA. The expression levels of CD81 protein in patient-tissue samples were determined by analyzing the immunohistochemistry images from normal and cancer tissues, which are stored in the HPA database. The IHC images were from tissue microarrays of patent samples (N = 208) from 20 cancer types. The bar chart was generated using the graphical interphase of HPA. The raw data can be downloaded from the HPA.

To determine whether there is a correlation between *SNCA* and *CD81* expression and melanoma-specific survival, we analyzed the skin cutaneous melanoma dataset from the TCGA PanCancer Atlas using cBioportal. The dataset contains the RNAseq data and the clinical features with outcomes. The Kaplan-Meier survival curve was constructed using the built-in survival analysis option of cBioportal [accessed on 2/25/24]. The high expression group was defined as the patient samples, in which the

expression of both *SNCA* and *CD81* mRNAs were 0.5z score higher than the mean expression value. The expression values were in RSEM units (RNAseq by Expectation Minimization). All the raw data can be obtained from cBioportal. Cytokine gene expression plots were created using GraphPad Prism v. 8 from the downloaded RNA-seq data from cBioportal [accessed on 3/20/2024].

Statistical Analyses and Software

All the statistical analyses were performed in GraphPad Prism v. 8. Experiments were performed for 3 biological replicates. Figures were prepared in Adobe Illustrator v. 6.

Results

Loss of α-syn expression in SK-MEL-28 melanoma cells causes a significant decrease in the level of the cell-surface tetraspanin CD81

The human cutaneous melanoma cell line SK-MEL-28, which is widely used and robustly expresses α-syn [10, 29], was used for this work. We previously engineered several SK-MEL-28 *SNCA*-knockout (*SNCA*-KO) clones. Lentivirus was used to re-express α-syn in some of the *SNCA*-KO clones, and such cells are referred to as *SNCA*-knock-in (*SNCA*-KI) cells. *SNCA*-KO and KI clones were also used.

This work was motivated to understand the cause of the reductions in motility, invasion, and migration in SK-MEL-28 *SNCA*-KO cells relative to control cells [20]. We attributed these effects to low levels of the adhesion protein L1CAM in the *SNCA*-KO cells, but we also wanted to determine if other proteins were involved. Because CD81 is involved in fusion events [21], invasion, migration [23, 25] and immune-signaling [21, 30], it was reasonable to test whether this protein was also downregulated in *SNCA*-KO clones. To this end, Western blotting revealed a significant reduction ($P = 0.0188$, $P = 0109$) in the level of CD81 in the lysates of *SNCA*-KO clones, KO8 and KO9, compared to control cells (Fig. 1A,B). The CD81 protein level significantly increased ($P = 0.04$) in KI9 cells compared to KO9 cells. The CD81 level increased in KI8 cells compared to KO8 cells, but the difference was not statistically significant (Fig. 1B). We validated this result in two additional *SNCA*-KO clones (KO11 and KO12), and both showed a decreased level of CD81 relative to the control cells (Fig S1A). Collectively, the results show a marked decrease in CD81 upon loss of α-syn expression in the melanoma line SK-MEL-28.

Because CD81 is commonly associated with EVs [22], we also isolated EVs from control, *SNCA*-KO, and *SNCA*-KI cells, and then characterized them by Western blotting for common EV-markers, i.e., CD81, CD9, CD63, HSP70 and HSP90 (Fig. 1C, S2A). We further characterized the EVs by NTA. The size distributions were mostly consistent with small EVs with negligible peaks for larger EVs, and there was no detectable cellular debris, which typically has a size of 2-5 μm [31] (Fig. S3A-E). Overall, the five EV-markers and size distributions were consistent with *bona fide* EVs. The results also showed a decreasing trend in two tetraspanins, CD81 and CD9, and an increasing trend in the tetraspanin CD63 in EVs from KO8 cells compared to the controls. A quantitative analysis of EV-proteins based on the sub-population of EVs was beyond the scope of this study and will be performed in future studies.

Correlation between *CD81* and *SNCA* in cancer

Based on our findings above with SK-MEL-28 cells, we predicted that *CD81* and *SNCA* would be positively correlated in melanoma patient samples and perhaps in other cancers. First, using cBioportal, we analyzed the RNAseq data from pooled patient samples across multiple cancer types. We found a significant moderate positive correlation between *CD81* and *SNCA* (Spearman R = 0.32, P = 1.86×10^{-29}) in the Pan-Cancer Analysis of Whole Genomes (PCAWG) dataset, which implicates the co-expression of *SNCA* and *CD81* in multiple cancers (Fig. 2A). Second, we asked which cancers exhibit a correlation between *SNCA* and *CD81*. Weak-to-moderate, and yet significant, positive correlations between *SNCA* and *CD81* were found in patient samples from pancreatic adenocarcinoma (PAAD) (Spearman R = 0.30, P = 4.712 x

10^{-5}) (Fig. 2B), invasive breast carcinoma (BRCA) (Spearman 0.20, P = 1.85 x 10^{-11}) (Fig. 2C), lung adenocarcinoma (LUAD) (Spearman R = 0.18, P = 6.929 x 10^{-5}) (Fig 2D), and cutaneous melanoma (SKCM) dataset (Spearman R = 0.23, P = 6.06 x 10^{-7}) (Fig, 2E). We conducted RT-qPCR analysis of SK-MEL-28 control and SK-MEL-28 *SNCA*-KO9 cells and found a significant decrease (41%, p = 0.0138) in *CD81* transcript level in KO9 cells compared to the control cells (Fig. 2F). This latter result is consistent with our bioinformatics analysis of patient samples, which shows a positive correlation between *CD81* and *SNCA* mRNA levels. Fig. S4 shows correlation analyses of cancers not shown in Fig. 2.

CD81 mRNA and protein levels in different cancers

To determine which cancer has the highest expression of *CD81* mRNA and protein, we first used the Human Protein Atlas (HPA) database to analyze RNAseq data from tumor samples from 17 different cancer types stored in TCGA. We found that *CD81* mRNA had the highest median expression (135.7 FPKM) in the melanoma tissue samples (N = 102) compared to 16 other cancer types (Fig. 3A). Second, we wanted to know the CD81 protein level in melanoma patient samples, and for that we accessed immunohistochemistry (IHC) data through human protein atlas (HPA). The IHCs were done using tissue microarray by the original submitters. 9 of the 12 (75%) melanoma tissue samples revealed medium to strong membranous staining for CD81 (antibody HPA007234) (Fig. 3B). These results support the idea that CD81 might be used as a prognostic biomarker or therapeutic target in melanoma.

CD81 and survival

To address whether the expression of *SNCA* and *CD81* impacted the survival of melanoma patients, we analyzed the RNAseq data from melanoma patient samples (N = 443) from the skin cutaneous melanoma (SKCM) dataset of the PanCancer atlas [32]. We found that melanoma-specific survival was significantly lower in patients with elevated mRNA levels of *CD81* only (median survival 65.9 months versus 138.8 months, $p = 0.0106$, $q = 0.0117$) (Fig 4A). Interestingly, survival was further decreased (median survival 61.15 months versus 138.80 months, $p = 1.873 \times 10^{-4}$, $q = 2.810 \times 10^{-4}$) in patients with elevated mRNA level of both or at least one of *SNCA* and/or *CD81* (Fig 4B).

CD81/SNCA and cytokines

To address whether decreased survival in patients with high expression of *SNCA* and *CD81* was associated with immunosuppression, we analyzed the mRNA expression of some key cytokine genes related to immune activation (*IFNG*, *CXCL13*) [33] and immune cell-mediated killing of cancer cells (*GZMB*, *PRF1*) [34]. In the same cohort of patients with decreased survival as described above (N = 174, 13 of these patients were not included in the survival study in Fig. 4B), we found a significantly lower mRNA expression of *IFNG* ($p = 2.29 \times 10^{-8}$, $q = 1.91 \times 10^{-7}$) (Fig. 4C), *CXCL13* ($p = 4.924 \times 10^{-6}$, $q = 2.155 \times 10^{-5}$) (Fig. 4D), *PRF1* ($p = 2.596 \times 10^{-4}$, $q = 7.381 \times 10^{-4}$) (Fig. 4E), and *GZMB* ($p = 4.288 \times 10^{-3}$, $q = 9.108 \times 10^{-3}$) (Fig. 4F). Taken together, these results suggest an inverse relation between *SNCA*/*CD81* and cytokine genes, i.e., patients with high expression of both *SNCA* and *CD81* have decreased expression of key cytokine

genes for immune activation and immune cell-mediated killing of melanoma cells, which can be associated with the decreased survival in this cohort. However, the cytokine profiling needs to be experimentally validated in in vitro or ex vivo model systems.

Discussion

In this work we found that the loss of α-syn expression in SK-MEL-28 melanoma cell line results in a significant decrease in the level of the tetraspanin CD81 (Fig. 1). We previously discovered that loss of α-syn expression in this cell line downregulates the levels of several cell-surface proteins, i.e., TfR1, L1CAM, FPN1 (ferroportin), N-Cadherin [20, 28]. We hypothesize that loss of α-syn expression causes the altered trafficking of some of these membrane proteins to the lysosome [20, 28], where they are degraded. We have observed a 40% decrease in the mRNA abundance of CD81 and an 83% decrease in CD81 protein levels in each KO clone. This suggests that α-syn might have a role in both the regulation of the mRNA level and the trafficking of CD81. Emerging evidence suggests that α-syn modulates mRNA stability [35] and transcription by interacting with the BAF complex in neuronal cells [36]. So, it is possible that α-syn is involved in modulation of CD81 at transcriptional, post-transcriptional and post-translational levels.

SK-MEL-28 *SNCA*-KO cells have significant defects in single-cell motility, invasion, and migration relative to control cells that express synuclein [20]. We reasonably concluded that these defects are a consequence of the *SNCA*-KO cells having a low level of L1CAM, which is a protein implicated in signaling, motility, and invasion [37, 38]. Given that *SNCA*-KO cells also have a significantly low level of CD81 relative to control cells, and that CD81 promotes the invasiveness of melanoma cells, we conclude that the decrease in the motility, invasion, and migration of *SNCA*-KO cells is a consequence of low levels of both CD81 and L1CAM. It is also possible that α-syn promotes invasion and migration of melanoma cells by inducing structural modification

of or changes in fluidity in the plasma membrane. Future work is necessary to clarify the mechanism.

An intriguing finding is that high levels of both *SNCA* and *CD81* mRNA correlate with an immunosuppressive mRNA signature (Fig. 4). This finding provides insights into the possible mechanism(s) of α-syn/*SNCA* involvement in melanoma pathogenesis. Based on our findings in Fig. 4, we propose that in a melanoma patient who has melanoma cells with elevated expression of the α-syn and CD81, these two proteins confer immunosuppression in the tumor microenvironment. Melanoma EVs are known to contribute to tumor-induced immune suppression in many ways [39, 40]. Mechanistically, one possibility is that the melanoma cells release extracellular vesicles containing α-syn and CD81 [41], and these vesicles with their differential cargo engage immune cells, such as monocytes/macrophages, natural killer (NK) cells, B cells, and CD4+/8+ T cells. These EVs may re-program immune cells to become suppressive regulatory cells [42, 43] or directly affect immune cells, leading to suppression of their anti-tumor functions associated with *GZMB*, *PRF1*, *CXCL13*, and *IFNG*. Emerging evidence suggests that CD81 promotes immunosuppression in mouse model of breast cancer [27] and targeting CD81 triggers killing of B cell lymphoma cells by macrophages and NK cells [44]. It has been shown that α-syn promotes inflammation and immune response in a mouse model of PD [45] and in the peritoneum [46]. We have recently reported that the SK-MEL-28 *SNCA*-KO clones secrete significantly more IL-1β and more IGFBP5 (Insulin growth factor binding protein 5) than the parental SK-MEL-28 cells [47], which implies that α-syn inhibits the secretion of these factors and thus has a role in immunomodulation. Future work will include mechanistic studies into how α-syn

modulates the cell surface expression of proteins and how α-syn modulates immune cell function in the tumor microenvironment.

Limitations

The databases that we used to analyze patient bulk RNAseq data from tumors did not contain single cell RNAseq data; instead, the RNAseq data we used was obtained from tumor tissue that contained a mixture of cells (tumor, fibroblasts, NK cells, CD4+ T helper cells, CD8+ cytotoxic T cells, and so on). Thus, our findings in Fig. 4 C-F regarding the immune modulators (*CXCL13*, *GZMB*, IFNG, *PRF1*) implicate immune cells like monocytes/macrophages, NK cells, B cells, and CD4+/8+ T cells as the source of the mRNA for these four genes. This is because these immune cells, but usually not melanoma cells, secrete factors such as granzyme B, interferon gamma, CXCL13, or perforin. Future work is required to test our predictions in *ex vivo* or *in vivo* model systems.

Acknowledgements

We thank the Feist-Weiller Cancer Center for providing seed funds to SNW for his melanoma work and for a Carroll Feist Predoctoral Fellowship award (149741440A) to NMA. We thank Dr. Andrew D. Yurochko for the gift of the actin primers and the staff of the LSUHS Research Core Facility for their help with the instruments used in this work.

Author contributions

Conceptualization: N.M.A., and S.N.W.; Investigation and data analysis: N.M.A., C.C., M.G., and S.N.W.; Project management: S.N.W.; Writing – original draft: N.M.A, and S.N.W.; Writing – review and editing: N.M.A., C.C., M.G., and S.N.W.

References

1. Kalia, L. V. & Lang, A. E. (2015) Parkinson's disease. *Lancet.* **386**, 896-912.

2. Hanahan, D. & Weinberg, R. A. (2011) Hallmarks of cancer: the next generation. *Cell.* **144**, 646-74.

3. Joon Yan Selene Lee, J. H. N., Seyed Ehsan Saffari, Eng-King Tan (2022) Parkinson's disease and cancer: a systematic review and meta-analysis on the influence of lifestyle habits, genetic variants, and gender. *Aging (Albany NY).* **14**, 2148-2173.

4. Gao, X., Simon, K. C., Han, J., Schwarzschild, M. A. & Ascherio, A. (2009) Family history of melanoma and Parkinson disease risk. *Neurology.* **73**, 1286-1291.

5. Bajaj, A., Driver, J. A. & Schernhammer, E. S. (2010) Parkinson's disease and cancer risk: a systematic review and meta-analysis. *Cancer Causes & Control.* **21**, 697-707.

6. Xinyuan Zhang, D. G., Niyaz Mohammadzadehhonarvar, & Xiqun Chen, X. G. (2021) Parkinson’s disease and cancer: a systematic review and meta-analysis of over 17 million participants. *BMJ Open.* 11:e046329.

7. Bose, A., Petsko, G. A. & Eliezer, D. (2018) Parkinson's Disease and Melanoma: Co-Occurrence and Mechanisms. *J Parkinsons Dis* **8**, 385-398.

8. Umber Dube, L. I., John P Budde, Bruno A Benitez, Albert A Davis, Oscar Harari, Mark M Iles, Matthew H Law, Kevin M Brown; 23andMe Research Team; Melanoma-Meta-analysis Consortium; Carlos Cruchaga (2020) Overlapping genetic architecture between Parkinson disease and melanoma. *Acta Neuropath* **139**, 347-364.

9. Agathe Quesnel, L. D. M., Chaimaa Tarzi, Vasileios P Lenis, Nathan Coles, Meez Islam, Claudio Angione, Tiago F Outeiro, Ahmad A Khundakar, Panagiota S Filippou (2024) Uncovering potential diagnostic and pathophysiological roles of α-synuclein and DJ-1 in melanoma. *Cancer Med* **13**, e6900.

10. Matsuo, Y. & Kamitani, T. (2010) Parkinson's Disease-Related Protein, alpha-Synuclein, in Malignant Melanoma. *Plos One* **5(5)**: e10481.

11. Weinreb, P. H., Zhen, W., Poon, A. W., Conway, K. A. & Lansbury, P. T. J. (1996) NACP, a protein implicated in Alzheimer's disease and learning, is natively unfolded. *Biochemistry* **35**, 13709-13715.

12. Chandra, S., Chen, X. C., Rizo, J., Jahn, R. & Sudhof, T. C. (2003) A broken alpha-helix in folded alpha-synuclein. *J Biol Chem* **278**, 15313-15318.

13. Kubo, S., Nemani, V. M., Chalkley, R. J., Anthony, M. D., Hattori, N., Mizuno, Y., Edwards, R. H. & Fortin, D. L. (2005) A combinatorial code for the interaction of alpha-synuclein with membranes. *J Biol Chem* **280**, 31664-31672.

14. Caughey, B. & Lansbury, P. T. (2003) Protofibrils, pores, fibrils, and neurodegeneration: Separating the responsible protein aggregates from the innocent bystanders. *Annu Rev Neurosci* **26**, 267-298.

15. Luk, K. C., Kehm, V., Carroll, J., Zhang, B., O'Brien, P., Trojanowski, J. Q. & Lee, V. M. (2012) Pathological alpha-synuclein transmission initiates Parkinson-like neurodegeneration in nontransgenic mice. *Science* **338**, 949-53.

16. Burre, J., Sharma, M., Tsetsenis, T., Buchman, V., Etherton, M. R. & Sudhof, T. C. (2010) alpha-Synuclein Promotes SNARE-Complex Assembly in Vivo and in Vitro. *Science* **329**, 1663-1667.

17. Logan, T., Bendor, J., Toupin, C., Thorn, K. & Edwards, R. H. (2017) alpha-Synuclein promotes dilation of the exocytotic fusion pore. *Nat Neurosci* **20**, 681-689.

18. Turriani, E., Lazaro, D. F., Ryazanov, S., Leonov, A., Giese, A., Schon, M., Schon, M. P., Griesinger, C., Outeiro, T. F., Arndt-Jovin, D. J. & Becker, D. (2017) Treatment with diphenyl-pyrazole compound anle138b/c reveals that alpha-synuclein protects melanoma cells from autophagic cell death. *Proc Natl Acad Sci USA.* **114**, E4971-E4977.

19. Pan, T., Zhu, J., Hwu, W.-J. & Jankovic, J. (2012) The Role of Alpha-Synuclein in Melanin Synthesis in Melanoma and Dopaminergic Neuronal Cells. *Plos One* **7(9)**:e45183.

20. Gajendran, N., Rajasekaran, S. & Witt, S. N. (2023) Knocking out alpha-synuclein in melanoma cells downregulates L1CAM and decreases motility. *Sci Rep* 13**(1)**:9243.

21. Hemler, M. E. (2003) Tetraspanin proteins mediate cellular penetration, invasion, and fusion events and define a novel type of membrane microdomain. *Annu Rev Cell Dev Biol* **19**, 397-422.

22. Escola, J. M., Kleijmeer, M. J., Stoorvogel, W., Griffith, J. M., Yoshie, O. & Geuze, H. J. (1998) Selective enrichment of tetraspan proteins on the internal vesicles of multivesicular endosomes and on exosomes secreted by human B-lymphocytes. *J Biol Chem* **273**, 20121-7.

23. Vences-Catalan, F., Rajapaksa, R., Kuo, C. C., Miller, C. L., Lee, A., Ramani, V. C., Jeffrey, S. S., Levy, R. & Levy, S. (2021) Targeting the tetraspanin CD81 reduces cancer invasion and metastasis. *Proc Natl Acad Sci USA.* **118(24)**:e2018961118.

24. Abu-Saleh, N., Kuo, C. C., Jiang, W., Levy, R. & Levy, S. (2023) The molecular mechanism of CD81 antibody inhibition of metastasis. *Proc Natl Acad Sci USA.* **120(26)**:e2305042120.

25. Hong, I. K., Byun, H. J., Lee, J., Jin, Y. J., Wang, S. J., Jeoung, D. I., Kim, Y. M. & Lee, H. (2014) The tetraspanin CD81 protein increases melanoma cell motility by up-regulating metalloproteinase MT1-MMP expression through the pro-oncogenic Akt-dependent Sp1 activation signaling pathways. *J Biol Chem* **289**, 15691-704.

26. Wang, H. X. & Hemler, M. E. (2015) Novel impact of EWI-2, CD9, and CD81 on TGF-beta signaling in melanoma. *Mol Cell Oncol* **2(1)**:e1030536.

27. Vences-Catalan, F., Rajapaksa, R., Srivastava, M. K., Marabelle, A., Kuo, C. C., Levy, R. & Levy, S. (2015) Tetraspanin CD81 promotes tumor growth and metastasis by modulating the functions of T regulatory and myeloid-derived suppressor cells. *Cancer Res* **75**, 4517-26.

28. Shekoohi, S., Rajasekaran, S., Patel, D., Yang, S., Liu, W., Huang, S. L., Yu, X. P. & Witt, S. N. (2021) Knocking out alpha-synuclein in melanoma cells dysregulates cellular iron metabolism and suppresses tumor growth *Sci Rep* **11(1)**:5267.

29. Lee, B. R., Matsuo, Y., Cashikar, A. G. & Kamitani, T. (2013) Role of Ser129 phosphorylation of alpha-synuclein in melanoma cells. *J Cell Sci* **126**, 696-704.

30. Levy, S. & Shoham, T. (2005) The tetraspanin web modulates immune-signalling complexes. *Nat Rev Immunol* **5**, 136-48.

31. Olander, M., Handin, N. & Artursson, P. (2019) Image-Based Quantification of Cell Debris as a Measure of Apoptosis. *Anal Chem* **91**, 5548-5552.

32. Ciriello, G., Miller, M. L., Aksoy, B. A., Senbabaoglu, Y., Schultz, N. & Sander, C. (2013) Emerging landscape of oncogenic signatures across human cancers. *Nat Genet* **45**, 1127-33.

33. Tirosh, I., Izar, B., Prakadan, S. M., Wadsworth, M. H., 2nd, Treacy, D., Trombetta, J. J., Rotem, A., Rodman, C., Lian, C., Murphy, G., et al. (2016) Dissecting the multicellular ecosystem of metastatic melanoma by single-cell RNA-seq. *Science* **352**, 189-96.

34. Ritter, A. T., Shtengel, G., Xu, C. S., Weigel, A., Hoffman, D. P., Freeman, M., Iyer, N., Alivodej, N., Ackerman, D., Voskoboinik, I., Trapani, J., Hess, H. F. & Mellman, I. (2022) ESCRT-mediated membrane repair protects tumor-derived cells against T cell attack. *Science.* **376**, 377-382.

35. Hallacli, E., Kayatekin, C., Nazeen, S., Wang, X. H., Sheinkopf, Z., Sathyakumar, S., Sarkar, S., Jiang, X., Dong, X., Di Maio, R., et al. (2022) The Parkinson's disease protein alpha-synuclein is a modulator of processing bodies and mRNA stability. *Cell* **185**, 2035-2056 e33.

36. Nakamura, T., Sugeno, N., Hasegawa, T., Ikeda, K., Yoshida, S., Ishiyama, S., Sato, K., Takeda, A. & Aoki, M. (2023) Alpha-synuclein promotes PRMT5-mediated H4R3me2s histone methylation by interacting with the BAF complex. *FEBS J*. **291(9)**:1892-1908.

37. Hoja-Lukowicz, D., Link-Lenczowski, P., Carpentieri, A., Amoresano, A., Pochec, E., Artemenko, K. A., Bergquist, J. & Litynska, A. (2013) L1CAM from human melanoma carries a

novel type of N-glycan with Gal beta 1-4Gal beta 1-motif. Involvement of N-linked glycans in migratory and invasive behaviour of melanoma cells. *Glycoconjugate J* **30**, 205-225.

38. Yang, M., Adla, S., Temburni, M. K., Patel, V. P., Lagow, E. L., Brady, O. A., Tian, J., Boulos, M. I. & Galileo, D. S. (2009) Stimulation of glioma cell motility by expression, proteolysis, and release of the L1 neural cell recognition molecule. *Cancer Cell Int* **9:27**, doi: 10.1186/1475-2867-9-27

39. Cheng, Y. C., Chang, Y. A., Chen, Y. J., Sung, H. M., Bogeski, I., Su, H. L., Hsu, Y. L. & Wang, H. D. (2021) The Roles of Extracellular Vesicles in Malignant Melanoma, *Cells.* **10**.

40. Hood, J. L. (2019) Natural melanoma-derived extracellular vesicles. *Semin Cancer Biol* **59**, 251-265.

41. Hurwitz, S. N., Rider, M. A., Bundy, J. L., Liu, X., Singh, R. K. & Meckes, D. G., Jr. (2016) Proteomic profiling of NCI-60 extracellular vesicles uncovers common protein cargo and cancer type-specific biomarkers. *Oncotarget.* **7**, 86999-87015.

42. Ahmadi, M., Abbasi, R. & Rezaie, J. (2024) Tumor immune escape: extracellular vesicles roles and therapeutics application, *Cell Commun Signal.* **22(1)**:9 doi: 10.1186/s12964-023-01370-3.

43. Zhou, Q., Yan, Y., Li, Y., Fu, H., Lu, D., Li, Z., Wang, Y., Wang, J., Zhu, H., Ren, J., et al. (2022) Tumor-derived extracellular vesicles in melanoma immune response and immunotherapy. *Biomed Pharmacother* **156**, 113790.

44. Vences-Catalan, F., Kuo, C. C., Rajapaksa, R., Duault, C., Andor, N., Czerwinski, D. K., Levy, R. & Levy, S. (2019) CD81 is a novel immunotherapeutic target for B cell lymphoma. *J Exp Med* **216**, 1497-1508.

45. Schonhoff, A. M., Figge, D. A., Williams, G. P., Jurkuvenaite, A., Gallups, N. J., Childers, G. M., Webster, J. M., Standaert, D. G., Goldman, J. E. & Harms, A. S. (2023) Border-associated macrophages mediate the neuroinflammatory response in an alpha-synuclein model of Parkinson disease. *Nat Commun* **14(1)**, 3754.

46. Alam, M. M., Yang, D., Li, X. Q., Liu, J., Back, T. C., Trivett, A., Karim, B., Barbut, D., Zasloff, M. & Oppenheim, J. J. (2022) Alpha synuclein, the culprit in Parkinson disease, is required for normal immune function. *Cell Rep* **38**, 110090.

47. Gadsden-Gray, J., Mukherjee, S., Ogunkua, O. & Das, S. K. (2012) Induction of neuronal damage in guinea pig brain by intratracheal infusion of 2-chloroethyl ethyl sulfide, a mustard gas analog. *J Biochem Mol Tox* **26**, 23-30.

48. Welsh, J. A., Goberdhan, D. C. I., O'Driscoll, L., Buzas, E. I., Blenkiron, C., Bussolati, B., Cai, H., Di Vizio, D., Driedonks, T. A. P., Erdbrugger, U., et al. (2024) Minimal information for studies of extracellular vesicles (MISEV2023): From basic to advanced approaches. *J Extracell Vesicles* **13**, e12404.

Legends

Fig. 1 The level of the tetraspanin protein CD81 is decreased in *SNCA*-KO cells. (A) Representative Western blots of CD81 and α-syn in cell lysates. An equal amount of protein was loaded into each lane, followed by SDS-PAGE, and Western blotting. (B) Quantification of band intensities. The band intensities were normalized to α-tubulin. Data are mean $\pm$ s.d. *P*-values were determined by one-way ANOVA with Tukey's post hoc test (N=3). (C) Characterization of EVs by Western blotting for common EV-markers.

Fig. 2 *CD81* expression is correlated with *SNCA* expression in multiple cancers. Bioinformatic analysis of RNAseq datasets suggests a weak to moderate correlation between the mRNA levels of *SNCA* and *CD81*. Correlation of *SNCA* and *CD81* mRNA expression from RNAseq data in (A) PCAWG (pan cancer analysis of the whole genome) dataset, N = 2922 samples from 2583 patients. (B) PAAD (Pancreatic Adenocarcinoma dataset from the TCGA, PanCancer Atlas), N = 177 (samples with mRNA data). (C) BRCA (Breast invasive Carcinoma dataset from TCGA, PanCancer Atlas), N = 1082 (samples with mRNA data). (D) LUAD (Lung Adenocarcinoma dataset from the TCGA, PanCancer Atlas), n= 510 (samples with mRNA data). (E) SKCM (Skin Cutaneous Melanoma dataset from the TCGA, PanCancer Atlas), N = 443 samples (samples with mRNA data). All correlation plots were generated by using the interactive platform of cBioportal and raw RNAseq data from the relevant datasets can be downloaded via cBioportal. Z-threshold=+/-0.1. RSEM=RNA-Seq by Expectation Maximization. (F) CD81 mRNA level is decreased in *SNCA*-KO melanoma cells. RT-

qPCR showing the relative fold change of *CD81* mRNA level in SK-MEL-28 control and *SNCA*-KO cells. N = 3 biological replicates. Student's paired t-test using GraphPad prism, version 8. Error bar, ± s.d. q = Benjamini-Hochberg parameter that estimates the false discovery rate.

Fig. 3 Bioinformatic analysis of TCGA data reveals that *the CD81* gene is highly expressed in melanoma patient samples. (A) *CD81* mRNA is highly expressed in tissue samples from melanoma patients. RNAseq data of 17 cancers from The Cancer Genome Atlas (TCGA) were analyzed using the Human Protein Atlas (HPA) portal. N = 102 (melanoma samples), N = 7932 (all tumor samples). (B) CD81 protein is commonly expressed in tissue samples of melanoma patients. Immunohistochemical analysis of melanoma patient samples were obtained from HPA. 9 out of 12 samples showed medium to high membranous staining for CD81 (High expression: 7, medium expression: 2, low expression:1, not detected: 2, N = 12). Tissue samples from some other cancers also showed staining for CD81 in varying degrees. CD81 antibody used by the submitter of this dataset was HPA007234.

Fig. 4 Melanoma-specific survival probability is decreased due to immunosuppressive cytokine gene expression profiling in patients with high expression of *SNCA* and *CD81* genes. (A) Melanoma-specific survival is decreased in patients with higher expression of *CD81*. Red line depicts melanoma patients with higher expression (above the median expression) of *CD81* (-0.31 - 5.17). Blue line depicts melanoma patients with lower expression (below the median expression) of CD81 (-1.53 - (-0.31). Median expression

= -0.31. N = 419, Low expression group = 211, high expression group= 208. (B) Melanoma-specific survival is decreased in patients with higher expression of at least one or both of *SNCA* and *CD81*. The red line depicts melanoma patients with high expression (Exp > 0.5 SD above the median expression) of at least one or both of *SNCA* and *CD81*. (N = 161, both high group = 39, *SNCA* only high group = 70, *CD81* only high group = 52), and the blue line depicts patients with low expression (Exp < 0.5 SD below the median expression) of at least one or both of *SNCA* and *CD81* (n=258). Z threshold =+/- 0.5. The total number of patients in the analysis, N = 419. Disease-specific survival option was chosen from cBioportal to generate K-M survival curve. (C-F) The expression of cytokine genes (*IFNG*, *CXCL13*, *PRF1, GZMB*) associated with immune-activation and immune-cell mediated killing of cancer cells were higher in patients with lower expression of *SNCA* and *CD81*. Patient groups: *SNCA-CD81* high: melanoma patients with high expression (Exp > 0.5 SD above than the median expression) of at least one or both of *SNCA* and *CD81* (n= 174, *SNCA* high 109, *CD81* high group = 91, both high = 26). *SNCA-CD81* low: melanoma patients with low expression (Exp < 0.5 SD below the median expression) of at least one or both of *SNCA* and *CD81* (N = 269)). Panels (B-F) focus on the same cohort of patients (N = 174) of which 13 patients were not included in the survival study by the study conductors. q = Benjamini-Hochberg estimate of false discovery rate. Red lines show the increase in the median values between groups.

Figure 1

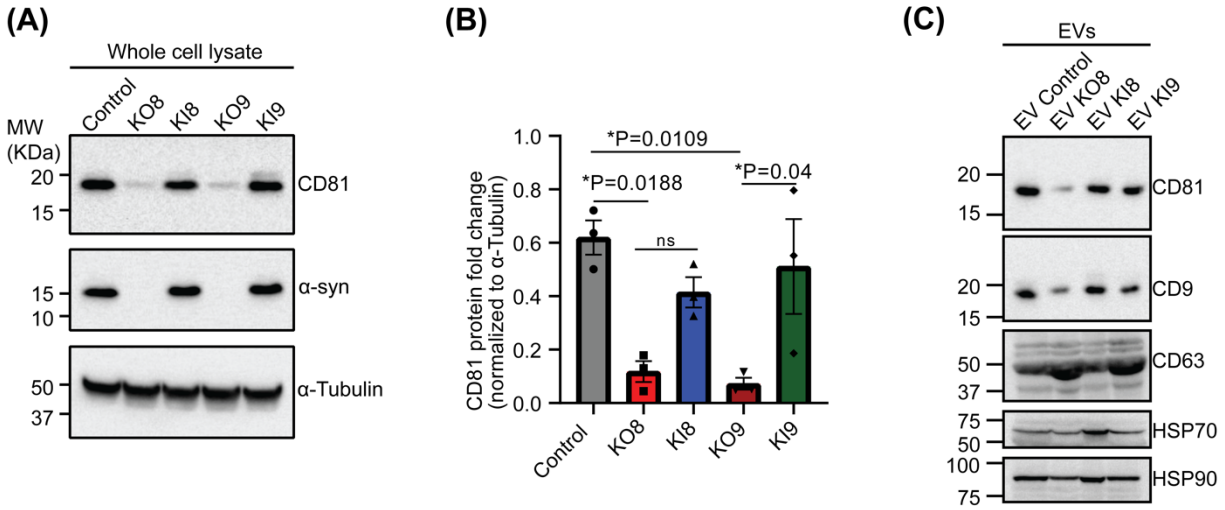
(A)
Whole cell lysate
Control
KO8
KI8
KO9
KI9
MW
(KDa)
20
15
CD81
15
10
α-syn
50
37
α-Tubulin
(B)
CD81 protein fold change
(normalized to α-Tubulin)
1.0
0.8
0.6
0.4
0.2
0.0
*P=0.0109
*P=0.0188
ns
*P=0.04
Control
KO8
KI8
KO9
KI9
(C)
EVs
EV Control
EV KO8
EV KI8
EV KI9
20
15
CD81
20
15
CD9
50
37
CD63
75
50
HSP70
100
75
HSP90

Figure 2

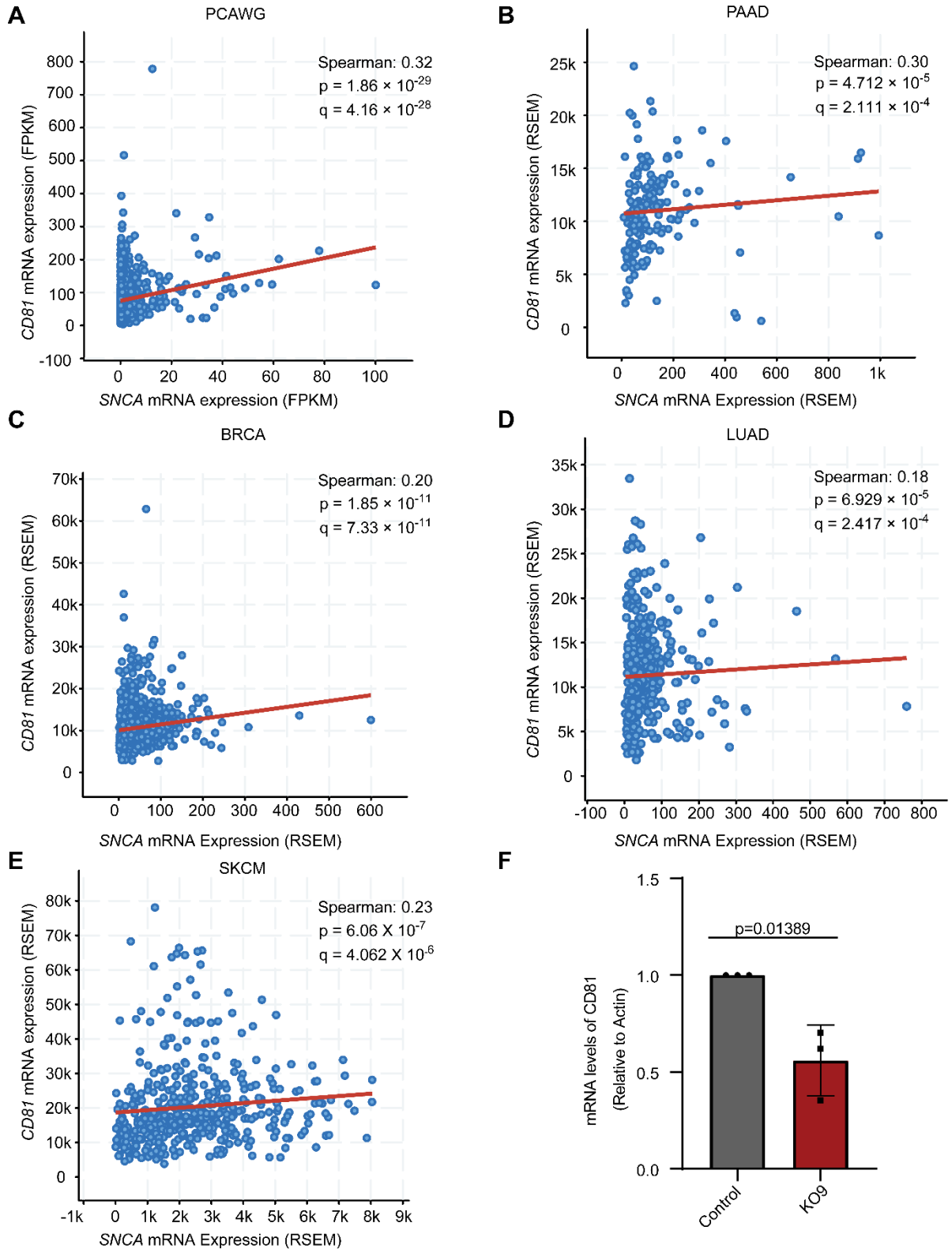
A
PCAWG
Spearman: 0.32
p = 1.86 × 10^-29
q = 4.16 × 10^-28
CD81 mRNA expression (FPKM)
SNCA mRNA expression (FPKM)
B
PAAD
Spearman: 0.30
p = 4.712 × 10^-5
q = 2.111 × 10^-4
CD81 mRNA expression (RSEM)
SNCA mRNA Expression (RSEM)
C
BRCA
Spearman: 0.20
p = 1.85 × 10^-11
q = 7.33 × 10^-11
CD81 mRNA expression (RSEM)
SNCA mRNA Expression (RSEM)
D
LUAD
Spearman: 0.18
p = 6.929 × 10^-5
q = 2.417 × 10^-4
CD81 mRNA expression (RSEM)
SNCA mRNA Expression (RSEM)
E
SKCM
Spearman: 0.23
p = 6.06 X 10^-7
q = 4.062 X 10^-6
CD81 mRNA expression (RSEM)
SNCA mRNA Expression (RSEM)
F
p=0.01389
mRNA levels of CD81
(Relative to Actin)
Control
KO9

Figure 3

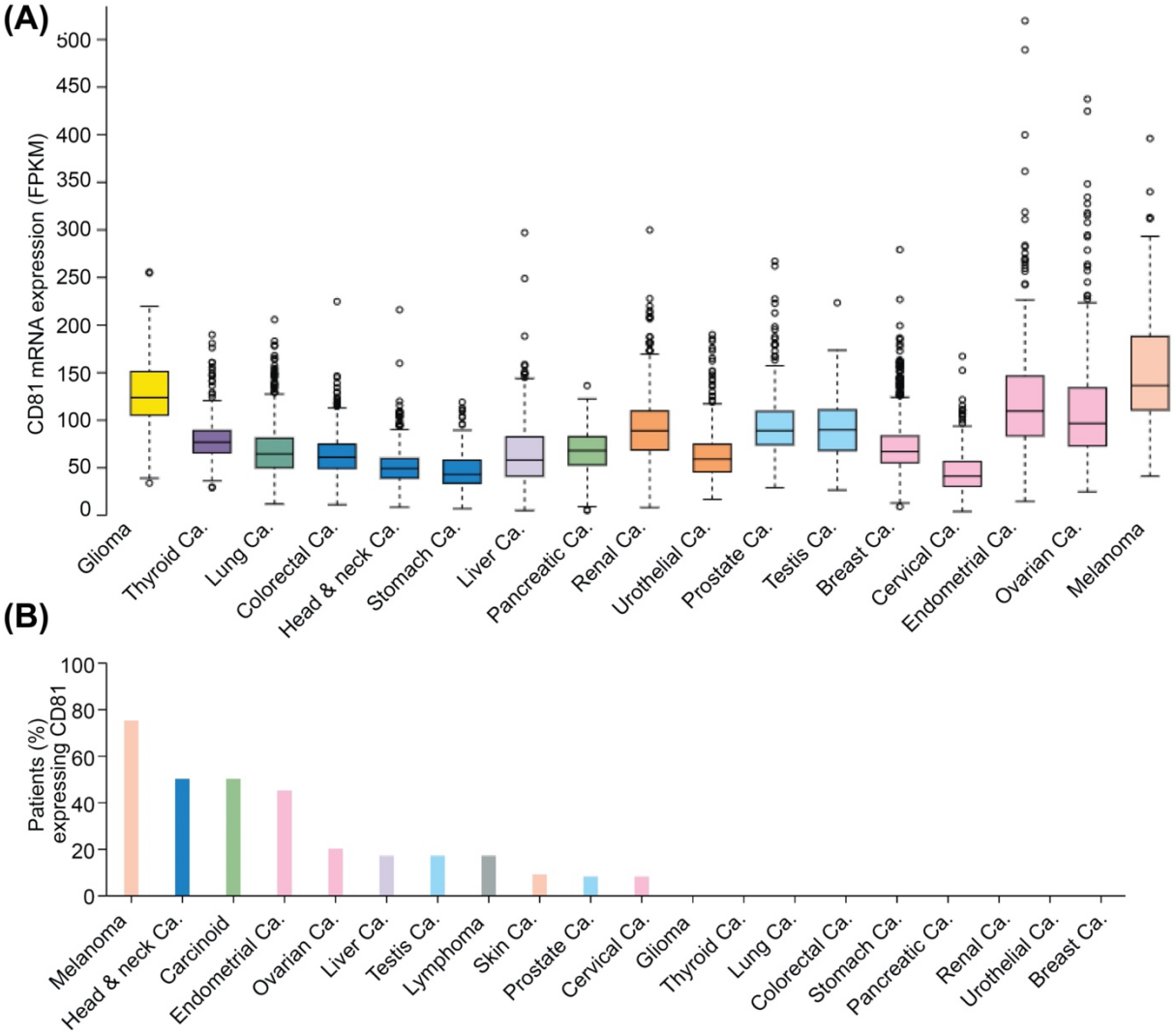
(A)
CD81 mRNA expression (FPKM)
500
450
400
350
300
250
200
150
100
50
0
Glioma
Thyroid Ca.
Lung Ca.
Colorectal Ca.
Head & neck Ca.
Stomach Ca.
Liver Ca.
Pancreatic Ca.
Renal Ca.
Urothelial Ca.
Prostate Ca.
Testis Ca.
Breast Ca.
Cervical Ca.
Endometrial Ca.
Ovarian Ca.
Melanoma
(B)
Patients (%) expressing CD81
100
80
60
40
20
0
Melanoma
Head & neck Ca.
Carcinoid
Endometrial Ca.
Ovarian Ca.
Liver Ca.
Testis Ca.
Lymphoma
Skin Ca.
Prostate Ca.
Cervical Ca.
Glioma
Thyroid Ca.
Lung Ca.
Colorectal Ca.
Stomach Ca.
Pancreatic Ca.
Renal Ca.
Urothelial Ca.
Breast Ca.

Figure 4

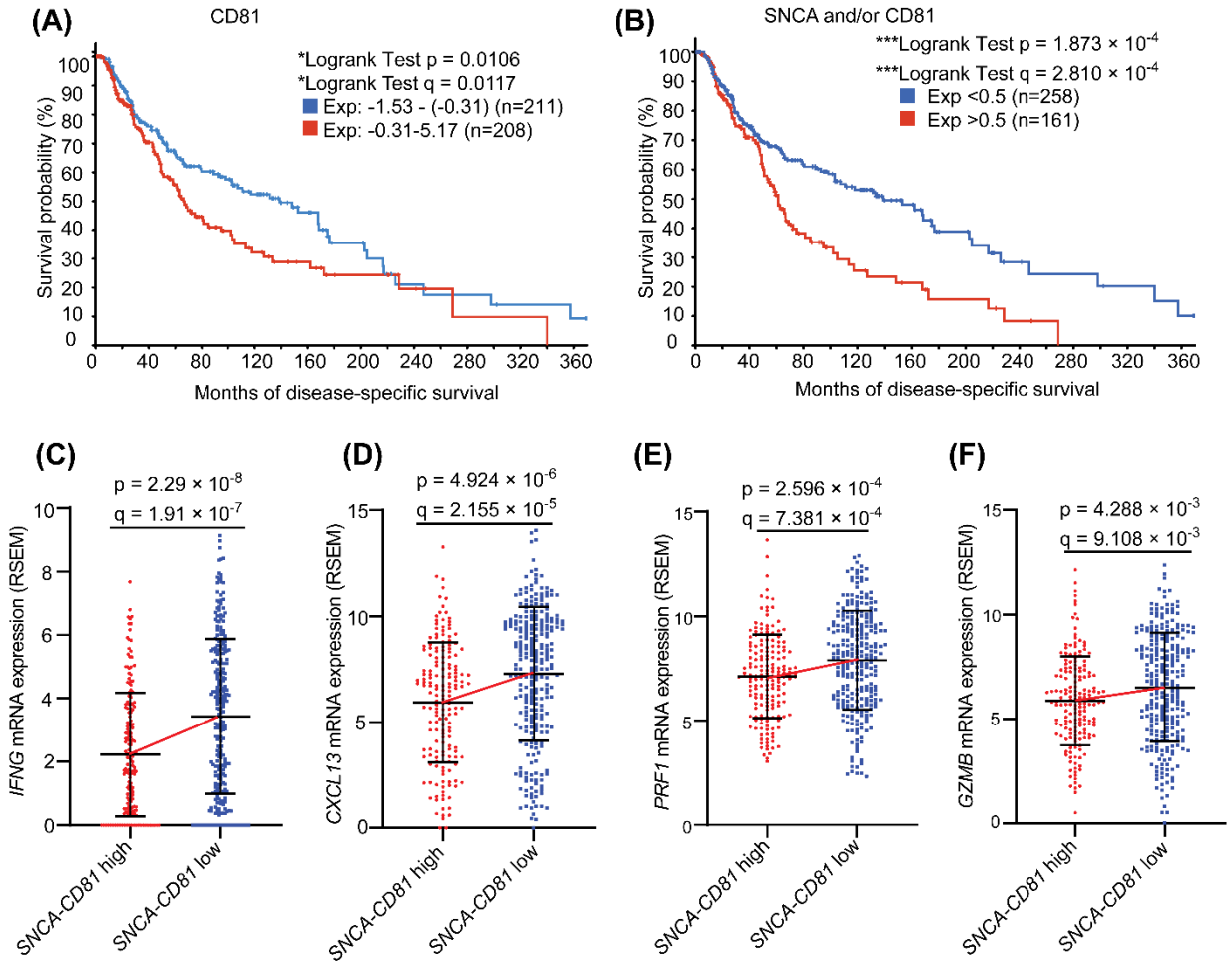
(A)
CD81
*Logrank Test p = 0.0106
*Logrank Test q = 0.0117
Exp: -1.53 - (-0.31) (n=211)
Exp: -0.31-5.17 (n=208)
Survival probability (%)
Months of disease-specific survival
(B)
SNCA and/or CD81
***Logrank Test p = 1.873 × 10-4
***Logrank Test q = 2.810 × 10-4
Exp <0.5 (n=258)
Exp >0.5 (n=161)
Survival probability (%)
Months of disease-specific survival
(C)
p = 2.29 × 10-8
q = 1.91 × 10-7
IFNG mRNA expression (RSEM)
SNCA-CD81 high
SNCA-CD81 low
(D)
p = 4.924 × 10-6
q = 2.155 × 10-5
CXCL13 mRNA expression (RSEM)
SNCA-CD81 high
SNCA-CD81 low
(E)
p = 2.596 × 10-4
q = 7.381 × 10-4
PRF1 mRNA expression (RSEM)
SNCA-CD81 high
SNCA-CD81 low
(F)
p = 4.288 × 10-3
q = 9.108 × 10-3
GZMB mRNA expression (RSEM)
SNCA-CD81 high
SNCA-CD81 low